EPJ Web of Conferences **182**, 02009 (2018) https://doi.org/10.1051/epjconf/201818202009
ICNFP 2017

Measurements of the *CP*-violating phase ϕ_s at LHCb

Varvara Batozskaya[1,a]
on behalf of the LHCb Collaboration

[1] *National Centre for Nuclear Research (NCBJ), Warsaw, Poland*

Abstract. The measurement of the mixing-induced *CP*-violating phase ϕ_s in the $B_s^0 - \bar{B}_s^0$ system is one of the key goals of the LHCb experiment. It has been measured at the LHCb collaboration exploiting the Run I data set and using several decay channels. In particular, the most recent Run I result has been obtained analyzing $B_s^0 \to J/\psi K^+K^-$ candidates in the mass region above the $\phi(1020)$ resonance. Despite the large improvements in the sensitivity of ϕ_s during the last decade, the precision is still limited by the available statistics.

1 Introduction

A primary goal of the LHCb experiment [1] (CERN) is the measurement of *CP* violation in quark sector. Our knowledge about *CP* violation is improved by comparison of the experimental results to the expected values of *CP*-violating parameters in search for deviations from the predictions. For decays which do not have a trivial phase space, amplitude analyses are essential for measurements of these parameters.

The *CP*-violating phase ϕ_s has been measured with several B_s^0 decay modes using 3 fb^{-1} of pp collisions collected by the LHCb experiment in 2011 and 2012 at $\sqrt{s} = 7$ TeV and 8 TeV, respectively. In this proceedings the review of the results and measurement methodology of these decays is reported. In addition, the future prospects on the possibility of observing *CP* violating parameters are dicussed.

2 *CP*-violating phase ϕ_s measurement

The interference between the mixing and direct decay of B_s^0 mesons to *CP* eigenstates allows to measure the *CP*-violating phase, ϕ_s, the average decay width, Γ_s and the decay width difference, $\Delta\Gamma_s$ between the lighter and heavier B_s^0 mass eigenstates (Fig. 1). Including only the dominant "tree level" contributions (Fig. 1), the phase ϕ_s within the Standard Model (SM) is predicted to be $-2\beta_s$ where $\beta_s = \arg(-V_{ts}V_{tb}^*/V_{cs}V_{cb}^*)$ [2]. An indirect determination of $2\beta_s = 0.0376^{+0.0008}_{-0.0007}$ rad is obtained using a global fit to experimental data [3].

Since the indirect determination of the phase ϕ_s is very precise in the SM, so-called New Physics effects, like new particles contributing to the $B_s^0 - \bar{B}_s^0$ mixing diagram, that modify the measured value can be revealed [4]. The measurement of *CP*-violating phase ϕ_s has independently been performed using $B_s^0 \to J/\psi K^+K^-$, $B_s^0 \to J/\psi\pi^+\pi^-$ and $B_s^0 \to \psi(2S)\phi$ decay channels.

[a] e-mail: varvara.batozskaya@cern.ch

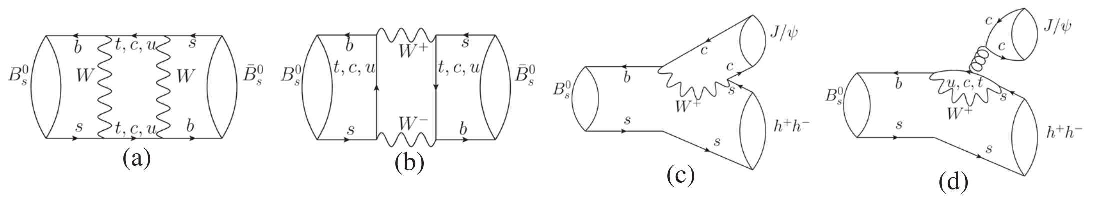

Figure 1. Feynman diagrams: (a-b) for $B_s^0 - \bar{B}_s^0$ mixing within the SM and contributing to the decay $B_s^0 \to J/\psi h^+h^-$ within the SM, where $h = \pi, K$: tree-level (c) and penguin (d) diagrams.

2.1 Analysis of the $B_s^0 \to J/\psi\phi$ decay

A tagged time-dependent angular fit to $B_s^0 \to J/\psi\phi$ candidates is applied to extract the *CP*-violating phase ϕ_s [5]. The final state of the decay is an admixture of *CP*-even states, $\eta_i = +1$ for $i \in \{0, \|\}$ and *CP*-odd states, $\eta_i = -1$ for $i \in \{\perp, \mathrm{S}\}$. It is decomposed into four amplitudes: three P-waves, A_0, $A_\|$, $A_\perp$ and one S-wave, A_S accounting for the nonresonant K^+K^- configuration. The phase ϕ_s is determined by $\phi_s = -\arg(\lambda)$ where $\lambda = \lambda_i/\eta_i$ and $\lambda_i = \frac{q}{p}\frac{\bar{A}_i}{A_i}$. In the absence of *CP* violation in decay, $\lambda = 1$. The complex parameters p and q describe the relation between mass and flavour eigenstates: $|B_{\mathrm{L,H}}\rangle = p|B_s^0\rangle \pm q|\bar{B}_s^0\rangle$ and $p^2 + q^2 = 1$.

The $B_s^0 \to J/\psi\phi$ candidates are reconstructed as the decay $J/\psi \to \mu^+\mu^-$ combined with a pair of oppositely charged kaons. After applying a full offline and trigger selection, 95690 ± 350 signal candidates of the $B_s^0 \to J/\psi\phi$ are obtained [5]. The decay time and angular acceptances, decay time resolution as well as efficiency of flavour tagging are taken into account in the fitting procedure. The decay time resolution is estimated using a large sample of prompt $J/\psi K^+K^-$ combinations produced directly in the pp interactions and is found to be 46 fs. Using a prescaled unbiased trigger sample and a tag and probe technique the decay time acceptance is determined from data. The angular acceptance is determined using simulated events that are subjected to the same trigger and selection criteria as the data. The flavour of the produced B_s^0 candidates is identified using two independent tagging algorithms: same side and opposite side. The flavour tagging algorithms are optimised on simulations and calibrated on data using flavour specific control channels. The combined effective tagging power is (3.73±0.15)% [5].

A weighted unbinned maximum likelihood fit is performed using a signal-only Probability Density Function (PDF), as described in Ref. [6]. The signal weights are extracted using the sPlot technique [7]. The data set is divided into six independent invariant K^+K^- mass bins that allows the measurement of the small S-wave amplitude in each bin and minimizes correction factors in the interference terms of the PDF [8]. The projections of the decay time and angular distributions are shown in Fig. 2. The final results are $\phi_s = -0.058 \pm 0.049 \pm 0.006$ rad, $\Gamma_s = 0.6603 \pm 0.0027 \pm 0.0015\ \mathrm{ps}^{-1}$ and $\Delta\Gamma_s = 0.0805 \pm 0.0091 \pm 0.0032\ \mathrm{ps}^{-1}$ where the first uncertainty is statistical and the second is systematic [5]. The dominant contribution to the systematic uncertainty is due to the decay time and angular efficiency and background subtraction.

2.2 Analysis of the $B_s^0 \to J/\psi\pi^+\pi^-$ decay

The analysis of $B_s^0 \to J/\psi\pi^+\pi^-$ decays has been also performed by the LHCb collaboration [9]. The decay is similar to the $B_s^0 \to J/\psi\phi$ one with a noticeable simplification: the final state being *CP*-odd, there is no need for the angular analysis. Five interfering $\pi^+\pi^-$ states dominated by $f_0(980)$ component are shown in Fig. 3. After trigger and selection chain 27100 ± 200 signal $B_s^0 \to J/\psi\pi^+\pi^-$ candidates

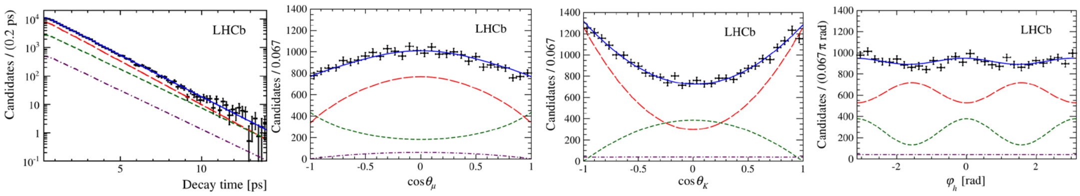

Figure 2. Decay time and angle distributions for $B_s^0 \to J/\psi\phi$ decays (black markers) with the one-dimensional projections of the PDF. The solid blue line shows the total signal contribution, which is composed of *CP*-even (long-dashed red), *CP*-odd (short-dashed green) and S-wave (dotted-dashed purple) contributions.

Figure 3. (left) Distribution of $m(\pi^+\pi^-)$ invariant mass with contributing components. (right) Invariant mass of $J/\psi\pi^+\pi^-$ combinations where the (red) solid curve shows the B_s^0 signal, the (brown) dotted line shows the combinatorial background, other colour lines indicate different reconstructed background contributions.

are reconstructed (Fig. 3). The decay time resolution is 40.3 fs and the combined effective tagging power is (3.89±0.25)%. With the time-dependent amplitude analysis, the measured value of the phase ϕ_s is 0.070±0.068±0.08 rad. The dominant systematic uncertainty is coming from knowledge about $\pi^+\pi^-$ resonance model. The combination of the $B_s^0 \to J/\psi\phi$ and $B_s^0 \to J/\psi\pi^+\pi^-$ fit results gives $\phi_s = -0.010 \pm 0.039$ rad [5].

2.3 Analysis of the $B_s^0 \to \psi(2S)\phi$ decay

Another B_s^0 decay mode with $\bar{b} \to \bar{c}c\bar{s}$ transition that has been exploited by the LHCb collaboration to measure the phase ϕ_s is $B_s^0 \to \psi(2S)(\to \mu^+\mu^-)\phi(\to K^+K^-)$ [10]. The formalism used for this analysis is very close to that of $B_s^0 \to J/\psi\phi$ decay [5] where the J/ψ meson is replaced with $\psi(2S)$. The number of signal candidates reconstructed from a fit to the data sample is ~4700 (Fig. 4). The decay time acceptance is determined using a control $B^0 \to \psi(2S)K^{*0}(\to K^+\pi^-)$ decay mode. Fig. 4 shows the decay time acceptance, which is defined as the product of the acceptance of the control channel and the ratio of acceptances of the simulated signal and control mode after full trigger and selection chain. The first measurement of the *CP*-violating parameters in a final state containing the $\psi(2S)$ resonance is $\phi_s = -0.23^{+0.29}_{-0.28} \pm 0.02$ rad, $\Gamma_s = 0.668 \pm 0.011 \pm 0.006$ ps^{-1} and $\Delta\Gamma_s = 0.066^{+0.041}_{-0.044} \pm 0.007$ ps^{-1}. The fit result is consistent with $B_s^0 \to J/\psi\phi$ measurement and the SM predictions. The systematic uncertainty is less than 20% of the statistical uncertainty, except for Γ_s where it is close to 60%.

2.4 Analysis of the $B_s^0 \to J/\psi K^+K^-$ decay in high $m(K^+K^-)$ range

The first measurement of the phase ϕ_s has been performed in the $B_s^0 \to J/\psi K^+K^-$ decay with K^+K^- invariant mass larger than 1050 MeV/c^2 [11] that is above the $\phi(1020)$ resonance region. This decay

Figure 4. Distribution of the $m(\psi(2S)K^+K^-)$ invariant mass for the selected $B_s^0 \to \psi(2S)\phi$ candidates and decay time acceptance in arbitrary units.

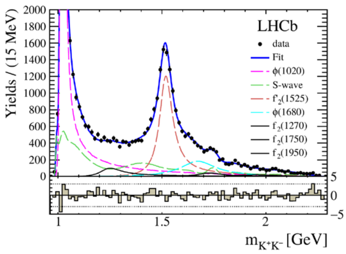

Figure 5. Distribution of the $m(J/\psi K^+K^-)$ invariant mass with contributing components.

has been studied using an analysis method very similar to that used for the $B_s^0 \to J/\psi\phi$ decay mode reported in Ref. [5]. The important difference between both decay analyses is that modelling of the $m(K^+K^-)$ distribution is included to distinguish different resonant and nonresonant contributions. The acceptance on the decay time is determined with the same method as described in Ref. [10] by using a control channel $B^0 \to J/\psi K^{*0}(\to K^+\pi^-)$. The K^+K^- mass spectrum is fitted by including the different contributions found in the time-dependent amplitude analysis as shown in Fig. 5. The final fit has been performed allowing eight independent sets of *CP*-violating parameters: three corresponding to $\phi(1020)$ transversity states, K^+K^- S-wave, $f_2(1270)$, $f_2'(1525)$, $\phi(1680)$ and the combination of the two high-mass $f_2(1750)$ and $f_2(1950)$ states. The *CP*-violating parameters measurement of $B_s^0 \to J/\psi K^+K^-$ in high $m(K^+K^-)$ region is $\phi_s = 0.119 \pm 0.107 \pm 0.034$ rad, $\Gamma_s = 0.650 \pm 0.006 \pm 0.004$ ps^{-1} and $\Delta\Gamma_s = 0.066 \pm 0.018 \pm 0.006$ ps^{-1}. The largest contribution to systematic uncertainty results from the resonance fit model. The combination with the B_s^0 decay fit results in the $\phi(1020)$ region gives $\phi_s = -0.025 \pm 0.045 \pm 0.008$ rad, $\Gamma_s = 0.6588 \pm 0.0022 \pm 0.0015$ ps^{-1} and $\Delta\Gamma_s = 0.0813 \pm 0.0073 \pm 0.0036$ ps^{-1} that improves a precision of the ϕ_s measurement by over 9%.

2.5 World average

The *CP*-violating phase and lifetime parameters have been measured by several experiments, namely four analyses using the $B_s^0 \to J/\psi\phi$ final state from CDF [12], D0 [13], ATLAS [14] and CMS [15] collaborations and five analyses using different final states performed by the LHCb collaboration, four of which discussed here. The world average result of ϕ_s and $\Delta\Gamma_s$ measurements from the Heavy Flavour Averaging Group [16] is shown in Fig. 6. They find $\phi_s = -0.021 \pm 0.031$ rad and $\Delta\Gamma_s = 0.085 \pm 0.006$ ps^{-1} that are dominated by the measurements from LHCb collaboration and are consistent with the SM predictions.

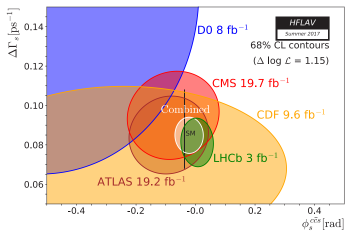

Figure 6. 68% confidence level regions in $\Delta\Gamma_s$ and ϕ_s plane obtained from individual contours of CDF, D0, CMS, ATLAS and LHCb measurements and the combined contour (solid line and shaded area) [16]. The expectation within the SM [3] is shown as a black thin rectangle.

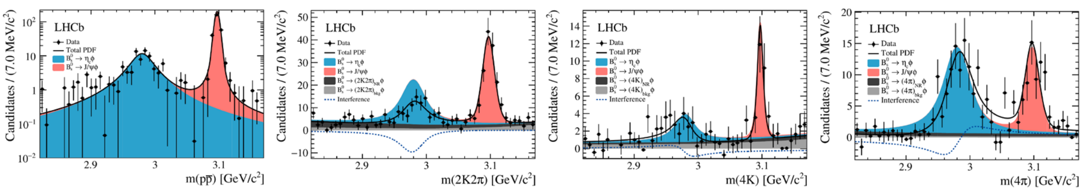

Figure 7. Invariant mass distributions for selected $p\bar{p}$, $K^+K^-\pi^+\pi^-$, $K^+K^-K^+K^-$ and $\pi^+\pi^-\pi^+\pi^-$ candidates.

2.6 Analysis of the $B_s^0 \to \phi\phi$ decay

The *CP*-violating phase has been measured by the LHCb collaboration in charmless $B_s^0 \to \phi(\to K^+K^-)\phi(\to K^+K^-)$ meson decays proceeding via a $b \to s\bar{s}s$ transition [17]. The decay is a pseudoscalar to vector-vector decay, but due to proximity of the ϕ resonance to that of the $f_0(980)$, there will also be contributions from S-wave and double S-wave processes. The $B_s^0 \to \phi\phi$ differential decay rate includes five polarization states: two *CP*-even, $\eta_i = +1$ for $i \in \{0, \parallel\}$ and three *CP*-odd, $\eta_i = -1$ for $i \in \{\perp, \mathrm{S}, \mathrm{SS}\}$. The *CP*-violating phase is determined to be $\phi_s = -0.17 \pm 0.15 \pm 0.03$ rad that is consistent with the theoretical predictions [18–20].

3 Future contributions for measuring ϕ_s

Other $b \to c$ or $b \to s$ processes with smaller branching fraction can be used to constraint ϕ_s. Future potential to the measurement of the phase ϕ_s from these decay modes is expected with data collected in Run II at $\sqrt{s}$=13 TeV.

3.1 Analysis of the $B_s^0 \to \eta_c\phi$ decay

For the first time the LHCb collaboration has observed the $B_s^0 \to \eta_c\phi$ decay mode, with $\eta_c \to K^+K^-\pi^+\pi^-$, $K^+K^-K^+K^-$, $\pi^+\pi^-\pi^+\pi^-$ and $p\bar{p}$ [21]. The J/ψ decay with the same final states is used as normalization mode. The interference between the η_c and purely nonresonant contributions is taken into account using an amplitude model to simultaneously fit the four hadrons and $p\bar{p}$ mass distributions (Fig. 7). The branching fraction is found to be $\mathcal{B}(B_s^0 \to \eta_c\phi) = [5.01 \pm 0.53(\mathrm{stat}) \pm 0.27(\mathrm{syst}) \pm 0.63(\mathcal{B})] \times 10^{-4}$ where the largest uncertainty is the one coming from the external branching ratio used for normalisation. First evidence for the $B_s^0 \to \eta_c\pi^+\pi^-$ decay mode has also been reported, with a branching fraction of $\mathcal{B}(B_s^0 \to \eta_c\pi^+\pi^-) = [1.76 \pm 0.59(\mathrm{stat}) \pm 0.12(\mathrm{syst}) \pm 0.29(\mathcal{B})] \times 10^{-4}$.

Figure 8. Distributions of $J/\psi\eta$ invariant mass and decay time for selected $B_s^0 \to J/\psi\eta$ decays. Combinatorial background (green), background from $B^0 \to J/\psi\eta$ decays (blue) and partially reconstructed background (orange) are shown.

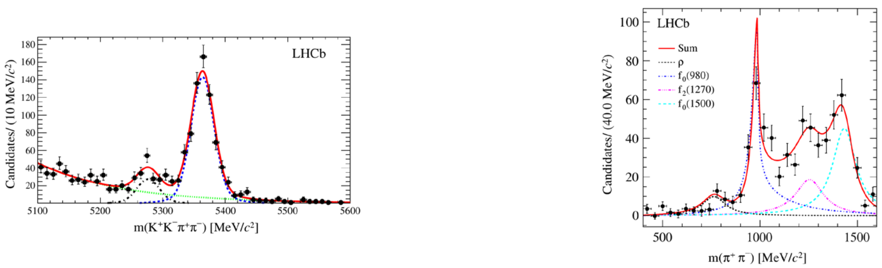

Figure 9. (left) Distribution of $K^+K^-\pi^+\pi^-$ invariant mass where the (blue) dashed line is the B_s^0 signal, the (green) dotted line shows the combinatorial background and the (black) dot-dashed line indicates the B^0 component. (right) Distributions of $\pi^+\pi^-$ invariant mass with contributing components.

3.2 Analysis of the $B_s^0 \to J/\psi\eta$ decay

The B_s^0 effective lifetime has been measured by the LHCb collaboration using *CP*-even $B_s^0 \to J/\psi\eta(\to \gamma\gamma)$ decay mode [22]. As ϕ_s is measured to be small and assuming *CP* conservation, the effective lifetime corresponds to Γ_L. Since the final state contains only two charged tracks, the invariant mass resolution is approximately 48 MeV/c^2 (Fig. 8), compared to ~8 MeV/c^2 for $B_s^0 \to J/\psi\phi$ decay. The effective lifetime for ~3000 signal candidates is measured to be $\tau_{\rm eff} = 1.479 \pm 0.034 \pm 0.011$ ps. The result is consistent with other *CP*-even lifetime measurements [23, 24].

3.3 Analysis of the $B_s^0 \to \phi\pi^+\pi^-$ decay

The first observation of the inclusive decay $B_s^0 \to \phi(\to K^+K^-)\pi^+\pi^-$ has been performed by the LHCb collaboration [25]. Fig. 9 shows the result of the final fit to the $m(K^+K^-\pi^+\pi^-)$ distribution. The B_s^0 yield is found to be ~700 events. Since the $\pi^+\pi^-$ spectrum includes several resonances, an amplitude analysis to the $\pi^+\pi^-$ mass and decay angle distributions is used to separate exclusive contributions to the B_s^0 meson decays (Fig. 9). The decays $B_s^0 \to \phi f_0(980)$, $B_s^0 \to \phi f_2(1270)$ and $B_s^0 \to \phi\rho^0$ are observed with a significance of 8σ, 5σ and 4σ evidence, respectively. The measurement of their branching fraction is $\mathcal{B}(B_s^0 \to \phi f_0(980)) = [1.12 \pm 0.16(\text{stat})^{+0.09}_{-0.08}(\text{syst}) \pm 0.11(\mathcal{B})] \times 10^{-6}$, $\mathcal{B}(B_s^0 \to \phi f_2(1270)) = ([0.61 \pm 0.13(\text{stat})^{+0.12}_{-0.05}(\text{syst}) \pm 0.06(\mathcal{B})] \times 10^{-6}$ and $\mathcal{B}(B_s^0 \to \phi\rho^0) = [2.7 \pm 0.7(\text{stat}) \pm 0.2(\text{syst}) \pm 0.2(\mathcal{B})] \times 10^{-7}$. The measurements are consistent with the SM predictions and, in case of the $B_s^0 \to \phi\rho^0$, it is provides a constraint on possible contributions from New Physics [26].

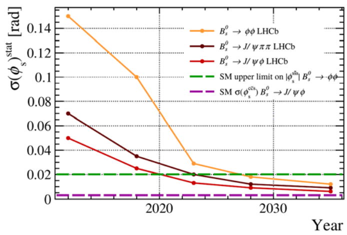

Figure 10. Projection of how precision on ϕ_s from LHCb measurements will scale as a function of time for different decay modes. Information taken from Ref. [27].

4 Summary

The most precise measurement of the *CP*-violating phase ϕ_s and lifetime parameters in the B_s^0 system has been performed using data collected by the LHCb experiment during Run I. So far all results are compatible with the Standard Model predictions. In order to reach an uncertainty of the measurement comparable or even better than the theoretical uncertainty of the SM prediction aside from improvements in available luminosity for the $B_s^0 \to J/\psi\phi$ channels, inclusion of new decay modes has been investigated. For example, the $B_s^0 \to J/\psi(\to e^+e^-)\phi$ channel not only could bring about 10% of the $\mu^+\mu^-$ mode statistics, but it will be also an important verification of the $B_s^0 \to J/\psi(\to \mu^+\mu^-)\phi$ as kinematics for both channels are expected to be identical. New $b \to c\bar{c}s$ decay modes have been investigated to either measure *CP* violating effects or make preparations for such measurements in the future. The evolition to the ϕ_s and $\phi_s^{s\bar{s}s}$ precision as a function of time for discussed decay modes is shown in Fig. 10. The statistical sensitivity of the ϕ_s measurement after the LHCb upgrade, with an integrated luminosity of 46 fb^{-1}, is expected to be ~0.01 rad, close to the present theoretical uncertainty [28]. As the measurement precision improves, the penguin polluion contributions to the B_s^0 decays have to been kept under control [29, 30].

Acknowledgments

I express my gratitude to the National Science Centre (NCN) in Poland for the financial support under the contract UMO-2015/17/N/ST2/04056. I would like to thanks the organizers of the ICNFP'2017 for the amazing atmosphere diring the conference in Crete and my LHCb colleagues who helped in the preparation of this talk.

References

[1] Alves Jr A A *et al.* (LHCb collaboration), JINST **3** (2008) S08005.

[2] Kobayashi M and Maskawa T, Prog.Theor.Phys. **49** (1973) 652; Cabbibo N, Phys.Rev.Lett. **10** (1963) 531.

[3] J. Charles *et al.*, Phys.Rev. **D91** (2015) no.7, 073007.

[4] Ligeti Z *et al.*, Phys.Rev.Lett. **97** (2006) 101801; Ball P and Fleischer R, Eur.Phys.J. **C48** (2006) 413; Lenz A, Phys.Rev. **D76** (2007) 065006; Fleischer R, ECONF **C0610161** (2006) 020; Nierste U, Int.J.Mod.Phys. **A22** (2007) 5986.

[5] Aaij R *et al.* (LHCb collaboration), Phys.Rev.Lett. **114** (2015) 041801.

[6] Xie Y, arXiv:0905.0724.

[7] Pivk M and Le Diberder F R, Nucl.Instrum.Methods Phys.Res., Sec.A **384** (2015) 491.

[8] Aaij R *et al.* (LHCb collaboration), Phys.Rev.Lett. **108** (2012) 241801.
[9] Aaij R *et al.* (LHCb collaboration), Phys.Lett. **B736** (2014) 186.
[10] R. Aaij *et al.* (LHCb Collaboration), Phys.Lett. **B762** (2016) 253.
[11] R. Aaij *et al.* (LHCb Collaboration), JHEP **1708** (2017) 037.
[12] Aaltonen T *et al.* (CDF collaboration), Phys.Rev.Lett. **109** (2012) 171802.
[13] Abazov V M *et al.* (D0 collaboration), Phys.Rev. **D85** (2012) 032006.
[14] G. Aad *et al.* (ATLAS Collaboration), JHEP **1608** (2016) 147.
[15] V. Khachatryan *et al.* (CMS Collaboration), Phys.Lett. **B757** (2016) 97.
[16] Y. Amhis *et al.*, arXiv:1612.07233 [hep-ex].
[17] R. Aaij *et al.* (LHCb Collaboration), Phys.Rev. **D90** (2014) no.5, 052011.
[18] M. Beneke, J. Rohrer and D. Yang, Nucl.Phys. **B774** (2007) 64.
[19] M. Bartsch, G. Buchalla and C. Kraus, arXiv:0810.0249 [hep-ph].
[20] H. Y. Cheng and C. K. Chua, Phys.Rev. **D80** (2009) 114026.
[21] R. Aaij *et al.* (LHCb Collaboration), JHEP **1707** (2017) 021.
[22] R. Aaij *et al.* (LHCb Collaboration), Phys.Lett. **B762** (2016) 484.
[23] R. Aaij *et al.* (LHCb Collaboration), Phys.Rev.Lett. **112** (2014) no.11, 111802.
[24] R. Aaij *et al.* (LHCb Collaboration), Phys.Lett. **B736** (2014) 446.
[25] R. Aaij *et al.* (LHCb Collaboration), Phys.Rev. **D95** (2017) no.1, 012006.
[26] L. Hofer, D. Scherer and L. Vernazza, JHEP **1102** (2011) 080.
[27] LHCb Collaboration (LHCb Collaboration), LHCb-PUB-2014-040.
[28] Aaij R *et al.* (LHCb collaboration) and Bharucha A *et al.*, Eur.Phys.J. **C73** (2013) 2373.
[29] R. Aaij *et al.* (LHCb Collaboration), JHEP **1511** (2015) 082.
[30] R. Aaij *et al.* (LHCb Collaboration), Phys.Lett. **B742** (2015) 38.